Surface Shortwave Radiative Fluxes derived from the US Air Force Cloud Depiction Forecast System World-Wide Merged Cloud Analysis

Rachel T. Pinker,[a] Wen Chen,[a] Yingtao Ma,[a] Sujay Kumar,[b] Jerry Wegiel,[b, c] Eric Kemp [b, d]

[a] Department of Atmospheric and Oceanic Science, University of Maryland, College Park, MD
[b] Hydrological Sciences Lab, NASA GSFC, Greenbelt, MD
[c] Science Applications International Corporation, McLean, VA
[d] Science Systems and Applications, Inc, Lanham, MD

Corresponding Author: pinker@atmos.umd.edu

ABSTRACT: We present a global scale evaluation of surface shortwave (SW↓) radiative fluxes as derived with cloud amount information from the US Air Force Cloud Depiction Forecast System (CDFS) II World-Wide Merged Cloud Analysis (WWMCA) and implemented in the framework of the NASA Land Information System (LIS). Evaluation of this product is done against ground observations, a satellite-based product from the Moderate Resolution Imaging Spectroradiometer (MODIS), and several reanalysis outputs. While the LIS/US Air Force (USAF) product tends to overestimate the SW↓ fluxes when compared to ground observations and satellite estimates, its performance is comparable or better than the following reanalysis products: ERA5, CFSR and MERRA-2. Results are presented using all available observations over the globe and independently for several regional domains of interest. When evaluated against ground observations over the globe the bias in the LIS/USAF product at daily time scale was about 9.34 Wm^{-2} and the rms was 29.20 Wm^{-2} while over the USA the bias was about 10.65 Wm^{-2} and the rms was 35.31 Wm^{-2}, respectively. The sample sizes used were not uniform over the different regions and the quality of both ground truth and the outputs of the other products may vary regionally. It is important to note that the LIS/USAF is a Near–Real-Time (NRT) product of interest for potential users and as such fills a need that is not met by most products. Due to latency issues, the level of observational inputs in the NRT product is less than in the reanalysis data.

KEYWORDS: USAF surface radiation; evaluation of LIS/USAF surface radiation; comparison

of LIS/USFA radiation with re-analysis model data.

SIGNIFICANCE STATEMENT: We evaluate a current scheme to produce surface radiative fluxes in the NASA Land Information System (LIS) framework as driven with cloud amount information from the US Air Force Cloud Depiction Forecast System (CDFS) II World-Wide Merged Cloud Analysis (WWMCA). The LIS/USAF product is provided at Near–Real-Time (NRT) and as such, fills a need that is not met by most products. Information used for evaluation are ground observations, Moderate Resolution Imaging Spectroradiometer (MODIS) satellite-based estimates, and independent outputs from several reanalysis. Since the various LIS products are used by the hydrometeorology community, this manuscript should be of interest to the users of the LIS/US Air Force (AF) information on surface radiative fluxes.

1. Introduction

Modeling land surface processes at global scale at high spatial resolutions is challenging. Efforts to do so have progressed gradually from models with time-fixed soil moisture to Bucket Models (Manabe 1969) with time- and space-varying soil moisture, to Big-Leaf models (Deardorff 1978) with explicit vegetation treatment, to the development of more sophisticated models including hydrological, biophysical, biochemical, ecological processes. Examples are the pioneering work of Sellers et al. (1986) who introduced the simple biosphere model (SiB), the Biosphere–Atmosphere Transfer Scheme (BATS) (Dickinson et al. 1993), the simplified Simple Biosphere model (SSiB) (Xue et al. 1991), and the Mosaic Model (Koster and Suarez 1992). The integration of land surface simulations, observation, and analysis methods to accurately determine land surface energy and moisture states led to such accomplishments as the 25 km Global Land Data Assimilation System (GLDAS) (Rodell et al. 2004) and the 12.5 km North American Land Data Assimilation System (NLDAS) (Mitchell et al. 2004). The NASA Land Information System (LIS) (Kumar et al. *2006*, 208a, 2008b, 2013*)* represents a step forward by taking advantage of technological improvements in implementing Land surface Models (LSMs) at high spatial resolution and by enabling land data assimilation (Arsenault et al. 2018). Consequently, the NASA LIS became a widely used land data assimilation system that runs several LSMs with observation-based on meteorology and remote sensing data to generate high quality estimates of land surface conditions. In LIS, land surface and atmosphere are linked to each other over a variety of time scales through the exchanges of water, energy, and carbon. An accurate representation of land surface processes is critical for improving models of the boundary layer and land/atmosphere coupling at all spatial and temporal scales and over heterogeneous domains. Configurations of LIS are used in operational environments at various agencies, including the US Air Force. Establishing the quality of the radiative forcing fields in LIS and their standing in respect to those from other well-established reanalysis models is a critical step in the development of improved representations of surface energy and water budget partitions.

The primary objective of this study is to evaluate a current NRT scheme in the LIS framework that produces surface radiative fluxes as driven with cloud information from the US Air Force Cloud Depiction Forecast System (CDFS) II World-Wide Merged Cloud Analysis (WWMCA) (D'Entremont et al., 2016) (LIS/USAF). This can serve as a basis for evaluating future modifications of the LIS/USAF product such as replacing the cloud amount information with Fields of Cloud Optical Depth (COD) from the same WWMCA system. For all the products used in this study the evaluation is done against ground observations at available sites. The primary tool used for comparisons at global scale is a satellite-based inference scheme described in Wang and Pinker (2009) with subsequent modifications as detailed in section 3.0. The inference scheme is driven with cloud optical parameters from the MODIS instrument on Terra and Aqua that are similar in nature to those that are generated by the US Air Force WWMCA product. The performance of the MODIS satellite product was first established against ground observations.

In section 2 we describe the current LIS/USAF scheme to derive surface SW↓ fluxes as driven with information on clouds from the WWMCA; in section 3 described is the UMD MODIS SW scheme; in section 4 we introduce the independent data used for comparison; results are shown in section 5 and a discussion and summary are provided in section 6.

2. Basics of the radiative model in the Air Force configuration of LIS

The methodology to derive surface SW↓ radiative fluxes in the LIS/USAF version is based on information from the Air Force cloud products using the approach described in Shapiro (1972). It is a statistical model tracing solar radiation through a reflecting and absorbing medium where the atmosphere is composed of **n** homogeneous layers. A flowchart illustrating the various steps is provided in **Figure 1.**

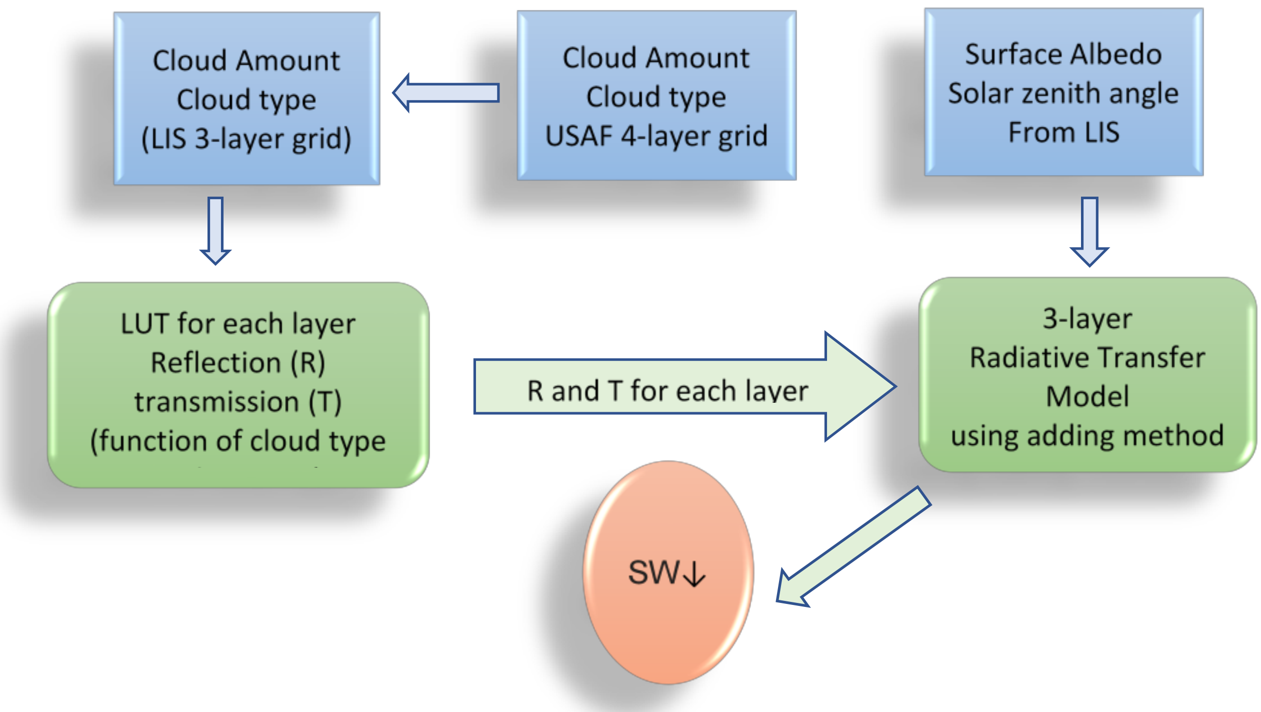

Fig. 1. A flowchart of the Shapiro (1976) model as implemented in the LIS/USAF NRT scheme.

The major components of the LIS/USAF scheme is a LUT for layer transmittance and reflectance and a 3-layer 2-flux radiative transfer solver based on adding method. The input WWMCA 4-layer cloud information is first converted to Shaprio's 3-layer setup. The layer transmittances and reflectanes of each layer are determined based on the layer cloud type and amount. Together with a surface albedo and solar angles as used in LIS modeling, the SW↓ can be computed analytically. Since the total solar radiation reaching the ground and reflected to space can be measured routinely, given a suitably sizeable series of such measurements under a variety of cloud conditions, the layer reflectivity and transmissivity can be estimated by a simple least-squares procedure. The downward flux of radiation leaving any layer is equal to the fractional transmission of that layer times the downward flux of radiation reaching that layer from above plus the fractional reflection of that layer times the upward flux of radiation reaching that layer from below. The system can be solved explicitly for radiation reaching the ground as a function of the vertically incident radiation and known or assumed reflection and transmission coefficients for each of the **n** layers and the ground surface with an assigned transmission and reflection coefficients for each cloud type. It can be used for any combination of cloud and cloud-free layers. Information on cloud amount and types is provided by the USAF World-Wide Merged Cloud Analysis (WWMCA) outputs (D'Entremont et al. 2016). As stated in Shapiro (1972) the approach is deliberately kept simple; however, the structure of the model permits progressive refinement. In this study, the 3-hourly averaged USAF product that covers the region bounded by: 59.875° S ~89.875° N, 179.875° W~179.875° E at 0.25° resolution (1440×600 points) has been used.

3. University of Maryland (UMD) MODIS SW↓ model

In the original version of the UMD MODIS model (Wang and Pinker 2009), a 1° surface SW↓ for all sky is computed in seven spectral intervals (0.2–0.4, 0.4–0.5, 0.5–0.6, 0.6–0.7, 0.7–1.19, 1.19–2.38, and 2.38–4.0 μm) assuming a plane-parallel, vertically inhomogeneous, scattering and absorbing atmosphere. Water vapor absorption is parameterized following the methods of Ramaswamy and Freidenreich (1992) and Chou and Suarez (1999). Ozone absorption in the ultraviolet wavelengths and in the visible wavelengths is computed following the approach of Lacis and Hansen (1974). The single-scattering properties and vertical profiles of aerosols were derived from the Optical Properties of Aerosols and Clouds (OPAC) software package (*Hess et al. 1998*). Five atmospheric aerosol vertical profiles (continental, desert, maritime, Arctic, and Antarctic) are used with the inference scheme. Cloud extinction coefficients, single-scattering albedos, and asymmetry factors are computed from the parameterizations of Edwards and Slingo (1996) for water clouds and from Chou et al. (2002) for ice clouds. Multiple scattering is dealt with by using the delta-Eddington approximation following the method of Joseph et al. (1976). Top-of-atmosphere solar spectral irradiance data are from MODerate resolution atmospheric TRANsmission3 (MODTRAN3). In the original MODIS inference scheme (Wang and Pinker 2009), the spectral reflectance for snow was assumed to be 0.9 and 0.6 for the visible and near-infrared parts of the spectrum, respectively. In the updated version, the surface spectral reflectance in the presence of snow is derived from a combination of snow-cover percentage and the MODIS surface spectral reflectance products, which are provided as 5-yr (2000–04) climatological statistics (the underlying surface types are aggregated according to the International Geosphere–

Biosphere Program classification (Moody et al. 2007). The model was further modified to facilitate the use of new information that became available, such as:

- MISR Level 3 monthly aerosol product (MIL3MAE or MIL3MAN)
- MODIS level3 weekly snow and ice product (MOD10C2 & MYD10C2)
- MODIS level3 daily snow and ice product (MOD10C1 & MYD10C1)
- Sea Ice Concentrations from Nimbus-7 SMMR and DMSP SSM/I-SSMIS Passive Microwave Data, Version 1, including both daily and monthly data and covering both North and South hemisphere.
- Precipitable water from the National Centers for Environmental Prediction (NCEP)-Department of Energy (DOE) daily reanalysis II.
- MODIS Aerosol Cloud Water Vapor Ozone Daily L3 Global 1° CMG (MOD08_D3 and MYD08_D3)

Auxiliary data prepared at UMD include land and sea mask, surface type, surface elevation, cloud layer thickness model coefficients, averaged albedo maps. A flowchart illustrating the entire process is presented in Figures 1 of Wang and Pinker (2009).

While the basic idea of the Shapiro (1972) model is similar to the UMD MODIS model (both are based on adding method for vertical quadrature) there are major differences that can be summarized as follows: 1). Shapiro (1972) model (SM) assumes only 3 layers of atmosphere, while the MODIS model has more than 40 layers, depending on the locations of clouds. 2). SM assumes that the whole solar spectral range is quasi-monochromatic or single band and gas absorption is crudely treated by choice of values assigned to the atmospheric layer absorptions, while the MODIS model has 7 bands and gas absorption is treated with a more detailed K-distribution method. 3). In SM, the quasi-monochromatic transmittance and reflectance of clouds are assigned based on climatological surface observations for various cloud types. The MODIS model has detailed parameterizations for the spectral cloud single scattering properties from Edwards and Slingo (1996) for water clouds and from Chou et al. (2002) for ice clouds. 4). Aerosol scattering and absorption, and molecular scattering are not explicitly included in the SM bur are in the MODIS model. 5). While being based on the 2-stream adding method, the SM does not divide the radiation into direct and diffuse components. Radiation is considered direct before encountering clouds, and as diffuse when transmitted through clouds.

4. Independent Data used for comparison

In addition to ground observations, we use satellite-based estimates and several well-known reanalysis products to evaluate the LIS/USAF SW↓ fluxes. The ground data are of primary importance in supporting the evaluation of all the other estimates used.

a. SURFRAD/BSRN data

The Baseline Surface Radiation Network (BSRN) is a project of the Data and Assessments Panel from the Global Energy and Water Cycle Experiment (GEWEX) under the umbrella of the World Climate Research Programme (WCRP) (Ohmura et al. 1998; Driemel et al. 2018) and as such is aimed at detecting important changes in the Earth's radiation field at the Earth's surface which may be related to climate changes. In 2004 the BSRN was designated as the global baseline network for surface radiation for the Global Climate Observing System (GCOS). The BSRN stations also contribute to the Global Atmospheric Watch (GAW). Since 2011 the BSRN and the Network for the Detection of Atmospheric Composition Change (NDACC) have reached a formal agreement to become cooperative networks. Twenty-four stations (**Table 1**) are available over the period 10/01/2013 to 08/31/2015 and used in this study. For several years the Surface Radiation (SURFRAD) Network (Augustine et al. 2000, Augustine et al. 2005; Augustine et al. 2013) was operated independently over the US. More recently, it became a part of the BSRN. Data can be downloaded from ftp://aftp.cmdl.noaa.gov/data/radiation/surfrad/. Instrument information can be found at https://www.esrl.noaa.gov/gmd/grad/surfrad/overview.html. The downloaded data are one-minute data, and written in ASCII format. Before the comparisons the data are processed to daily averages. Missing values are filled by the closest values as a function of solar zenith angle.

Table 1. Global BSRN sites used in the evaluation of SW↓ from the various products.

Station full name	Abbreviation	Location	Lat	Lon	Surface type	Topography type	Rural/Urban II
Bondville	BON	Illinois, U.S.	40.07	-99.37	grass	flat	rural
Desert Rock	DRA	Nevada, U.S.	36.63	-116.02	desert	flat	rural
Fort Peck	FPK	Montana, U.S.	48.31	-105.10	grass	flat	rural

Goodwin Creek	GWN	Mississippi, U.S.	34.25	-89.87	grass	hilly	rural
Penn. State Univ.	PSU	Pennsylvania, U.S.	40.72	-77.93	cultivated	mountain valley	rural
Sioux Falls	SXF	South Dakota, U.S.	43.73	-96.62	grass	hilly	rural
Table Mountain	TBL	Colorado, U.S.	40.12	-105.24	grass	flat	rural
Alice Springs	ASP	Australia, Northern Territory	-23.80	133.89	grass	flat	rural
Cocos Island	COC	Australia, Cocos (Keeling) Islands	-12.19	96.84	grass	flat	rural
Darwin Met Office	DWN	Australia	-12.42	130.89	grass	flat	rural
Brasilia	BRB	Brazil, Brasilia City	-15.60	-47.71	Concrete/shrub	flat	rural
Petrolina	PTR	Brazil	-9.07	-40.32	Concrete/shrub	flat	rural
São Martinho da Serra	SMS	Brazil	-29.44	-53.82	Concrete/grass	flat	rural
Cabauw	CAB	Netherlands	51.97	4.93	grass	flat	rural
Camborne	CAM	United Kingdom	50.22	-5.32	grass	flat	rural
Carpentras	CAR	France	44.08	5.06	cultivated	hilly	rural
Cener	CNR	Spain, Navarra	42.82	-1.60	asphalt	mountain valley	urban
Izaña	IZA	Spain, Tenerife	28.31	-16.50	rock	mountain top	rural
Lindenberg	LIN	Germany	52.21	14.12	cultivated	hilly	rural
Palaiseau, SIRTA Observatory	PAL	France	48.71	2.21	concrete	flat	urban

Payerne	PAY	Switzerland	46.82	6.94	cultivated	hilly	rural
Sonnblick	SON	Austria	47.05	12.96	rock	mountain top	rural
Xianghe	XIA	China	39.75	116.96	desert, rock	flat	rural
Gobabeb	GOB	Namibia, Namib Desert	-23.56	15.04	desert gravel	flat	rural
Tamanrasset	TAM	Algeria	22.7903	5.5292	desert, rock	flat	rural

b. ARM/SGP C1 site

The Southern Great Plains (SGP) atmospheric observatory was the first field measurement site established by the Atmospheric Radiation Measurement (ARM) user facility (*Stokes and Schwartz* 1994). This observatory is the world's largest and most extensive climate research facility (https://www.arm.gov/capabilities/observatories/sgp). The Central location (C1) is 36.61° N, 97.49° W. The data are available from https://www.arm.gov/capabilities/observatories/sgp

c. *The European Centre for Medium-Range Weather Forecasts (ECMWF) Reanalysis v5 (ERA5)*

The European Centre for Medium-Range Weather Forecasts (ECMWF) Reanalysis v5 (ERA5) is the fifth generation of the European Centre for Medium-Range Weather Forecasts (ECMWF) re-analysis for the global climate and weather for the past 4 to 7 decades (Hersbach et al. 2018). Currently data are available from 1950, split into Climate Data Store entries for 1950-1978 (preliminary back extension) and from 1979 onwards (final release plus timely updates). ERA5 replaces the ERA-Interim re-analysis. Re-analysis combines model data with observations from across the world into a globally complete and consistent dataset. ERA5 provides hourly estimates for a large number of atmospheric, ocean and land-surface quantities. The data are re-gridded to a regular latitude/longitude grid of 0.25° for the re-analysis. In this study we use the "ERA5 hourly data on single levels from 1979 to present". The data are available at: https://cds.climate.copernicus.eu/cdsapp#!/dataset/reanalysis-era5-single-levels?tab=overview *d.* The Climate Forecast System Reanalysis (CFSR)

The Climate Forecast System Reanalysis (CFSR) (Saha et al. 2010, *2014*) is a third-generation reanalysis product developed by NOAA National Centers for Environmental Prediction (NCEP). It is a global, high resolution, coupled atmosphere-ocean-land surface - sea ice system designed to provide the best estimate of the state of these coupled domains over this period. Here we used the 6-hourly product with a spatial resolution of 0.5°×0.5°. The data are available at: https://climatedataguide.ucar.edu/climate-data/climate-forecast-system-reanalysis-cfsr

e. The Modern-Era Retrospective analysis for Research and Applications (MERRA)

The Modern-Era Retrospective analysis for Research and Applications, Version 2 (MERRA-2) (Gelaro et al. 2017) is a global atmospheric reanalysis developed by NASA's Global Modeling and Assimilation Office (GMAO) providing data from 1980 on. It replaces the original MERRA data because of the advances made in the assimilation system that enable assimilation of modern hyperspectral radiance and microwave observations, along with GPS-Radio Occultation datasets. It also uses NASA's ozone profile observations that began in late 2004. Additional advances in both the GEOS model and the GSI assimilation system are included in MERRA-2. The data center for MERRA-2 provides DOI and a full citation for all the MERRA-2 data. For the 1 hourly radiation: Global Modeling and Assimilation Office (GMAO) (2015), MERRA-2 tavg1_2d_rad_Nx: 2d,1-Hourly, Time-Averaged,Single-Level,Assimilation, Radiation Diagnostics V5.12.4, Greenbelt, MD, USA, Goddard Earth Sciences Data and Information Services Center (GES DISC), Accessed: [Data Access Date], 10.5067/Q9QMY5PBNV1T. The data are available at: https://gmao.gsfc.nasa.gov/reanalysis/MERRA-2/).

5. Results

a. Issues related to homogeneity of data products

Before conducting the comparison, all products are re-gridded (linear interpolation) to 1° resolution and converted to daily values; they are cropped to the domain of 59.5° S~59.5° N as used in LIS. The spatial matching is done by using the estimations (daily data) at the nearest points for each site location. If the number of nearest points is more than 2, than the estimation is the mean values with the weights of latitude and longitude.

Several aspects of the comparison process itself can introduce errors that are difficult to estimate. For instance, each model was produced at different spatial and temporal scales. In the comparisons, all data were scaled to 1° spatial resolution and to daily time scales. LIS/USAF provides data averaged for each 3-hourly interval. The daily value is obtained by simply averaging the 3-hourly mean product for both ERA5 and MERRA-2. For CFSR, the daily values are obtained by averaging the 6-hourly mean products. The satellite UMD/MODIS product is based on two observations per day. The procedure to obtain a daily average is described in detail in Wang and Pinke*r* (2009). It will be recaptured here briefly.

The diurnal variation of SW↓ is caused mainly by clouds and position of the Sun. The latter can be well described, but the diurnal variation of clouds is not readily available. Using MODIS observations from both Terra and Aqua to estimate SW↓, a difference between morning and afternoon fluxes was observed. Over most of the continents, SW↓ fluxes are larger in the morning than in the afternoon (over much of the oceans, the differences are reversed). Over land there are more clouds in the afternoon. The diurnal cycle of clouds drives the surface SW↓ cycle (Chen and Houze, 1997; Duvel, 1989; Gray and Jacobson, 1977). The combination of MODIS observations from Terra and Aqua provides an opportunity to construct realistic daily values. The daily average is computed by assuming that MODIS observations from Terra at 1030 LT and from Aqua at 1330 LT represent the atmospheric conditions from sunrise to local noon and from local noon to sunset, respectively. The diurnal variation of incident fluxes will be dictated only by the incident solar flux at top of the atmosphere which is determined by the cosine of the solar zenith angle. The daily integration of radiative fluxes is reduced to the integration of the cosine of the solar zenith angle. Thus, the daily average radiative flux is calculated as follows:

$$Flux_{daily} = \left(\int_{Sunrise}^{Noon} Flux(\mu(t))dt + \int_{Noon}^{Sunset} Flux(\mu(t)dt) \right) / 24 \text{ hours},$$

where Flux(μ(t)) is instantaneous radiative flux at time **t** with cosine of solar zenith angle μ(t).

Another issue related to the accuracy of SW↓ fluxes as derived from satellite observations is related to the nonlinearity of the relationship between radiance and flux. In most cases, provided are radiances averaged at a certain scale and these are used to compute the flux.

b. Evaluation against Ground Observations

Observations from the BSRN network are available over numerous global sites. The ARM/SGP C1 site is considered a super site in terms of quality and scope of observations. Evaluation will be done using all available data. Since the performance of LIS/USAF product over different regions is of interest, the evaluation will also be presented independently over the US and Europe, where several observing sites are available. Results for Brazil, Australia, Africa and China (with a limited number of ground sites) will be provided in a Supplement.

1) EVALUATION USING ALL GLOBALLY DISTRIBUTED SITES

Evaluation of daily SW↓ from UMD/MODIS, LIS/USAF, ERA5, CFSR and MERRA-2 against ground observations (all available sites as illustrated in **Figure 2**) during 10/01/2013 – 08/31/2015 has been performed.

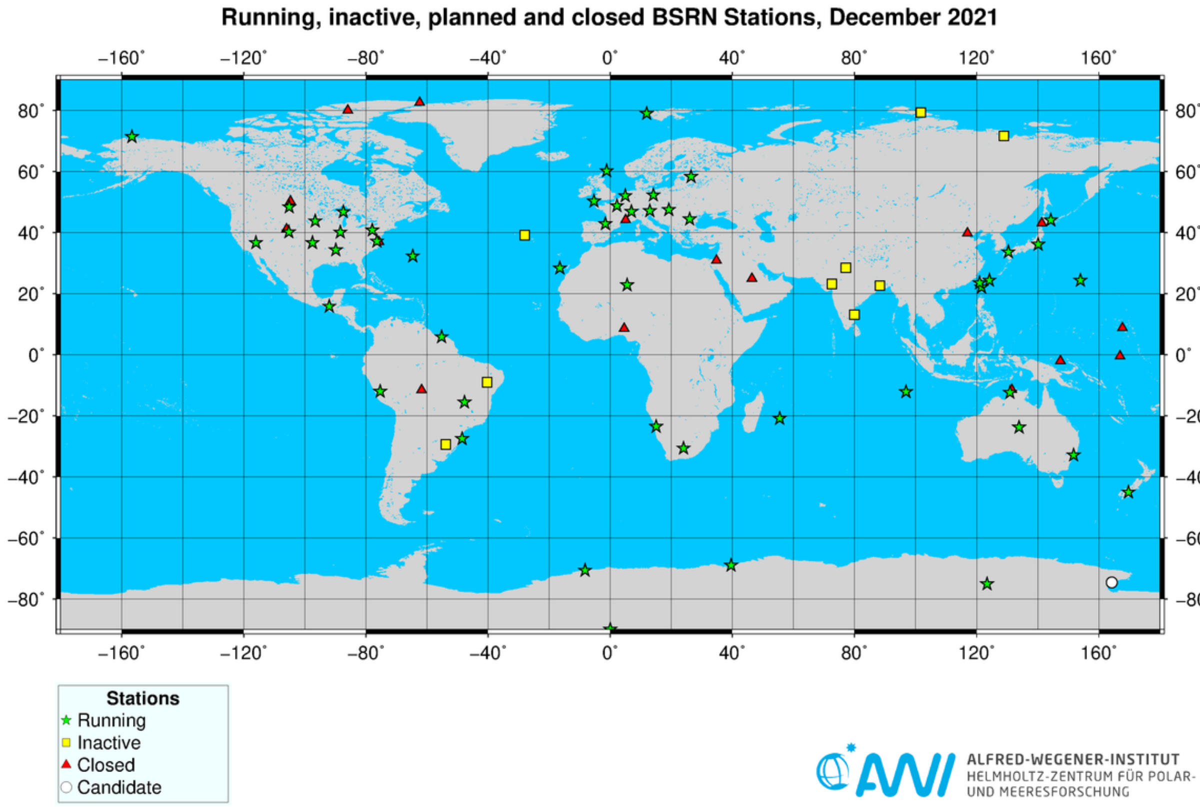

Fig. 2. Global distribution of BSRN sites.

As seen from **Table 2** in best agreement with ground observations are the results from UMD MODIS and ERA5. In terms of lowest bias LIS/USAF are close to each other while the RMSE for LIS/USAF is much lower than CFSR. To get a better insight on possible reasons for the observed differences one could segregate the data by season, latitude or land use type. It is well known that cloud detection is not uniform for different cloud conditions and over different surface types (dark or bright). The movement of clouds within the interval of observations or prediction time steps has an impact on the results. The record length used in this study and the limited number of ground observations are not conducive to such separations. While for understanding differences, such analysis may be helpful, most users are interested in the overall agreement in deciding which data they prefer rather than seasonal or latitudinal differences.

To understand the reasons for differences among products is very difficult. While the key features of the LIDS/USAF and UMD MODIS have been discussed, the reasons for differences between the reanalysis products are numerous such the observing system, data assimilation (DA) system, model components and post processing system. As documented for ERA5 (https://confluence.ecmwf.int/display/CKB/ERA5%3A+data+documentation), it is produced using 4D-Var data assimilation and model forecasts in CY41R2 of the ECMWF Integrated Forecast System (IFS), with 137 hybrid sigma/pressure levels in the vertical. The atmospheric model in the IFS is coupled to a land-surface model (HTESSEL) and an ocean wave model (WAM).

The CFSRv2 (Saha et al., 2014) is produced by the second version of the NCEP Climate Forecast System (CFSv2) which uses 3D-Var DA system, and coupled atmosphere-ocean-land surface-sea ice system. The horizontal resolution is ~38 km (T382) with 64 levels in the vertical. The global ocean is 0.25° at the equator, extending to a global 0.5° beyond the tropics, with 40 levels. The global land surface model has 4 soil levels and the global sea ice model has 3 levels.

The MERRA-2 (R. Gelaro et al., 2017) is produced with version 5.12.4 of the GEOS atmospheric data assimilation system (GSI 3D-Var). The key components of the system are the GEOS atmospheric model (Rienecker et al. 2008; Molod et al. 2015) and the GSI analysis scheme (Wu et al. 2002; Kleist et al. 2009). The model includes the finite-volume dynamical core of Putman and Lin (2007), which uses a cubed-sphere horizontal discretization at an approximate resolution of 0.5° × 0.625° and 72 hybrid-eta levels from the surface to 0.01 hPa. The analysis is computed on a latitude–longitude grid at the same spatial resolution as the atmospheric model using a 3DVAR algorithm based on the GSI with a 6-h update cycle and the so-called FGAT procedure for computing temporally accurate observation-minus-background departures. The analysis is applied as a correction to the background state using an IAU procedure (Bloom et al. 1996). As such, to pinpoint the reasons for observed differences in the predicted SW↓ from these models is beyond the scope of this study.

In the following, independent evaluation over the US and Europe will be presented. Independent results over Brazil, Australia, Africa and China are presented in the **Supplement.**

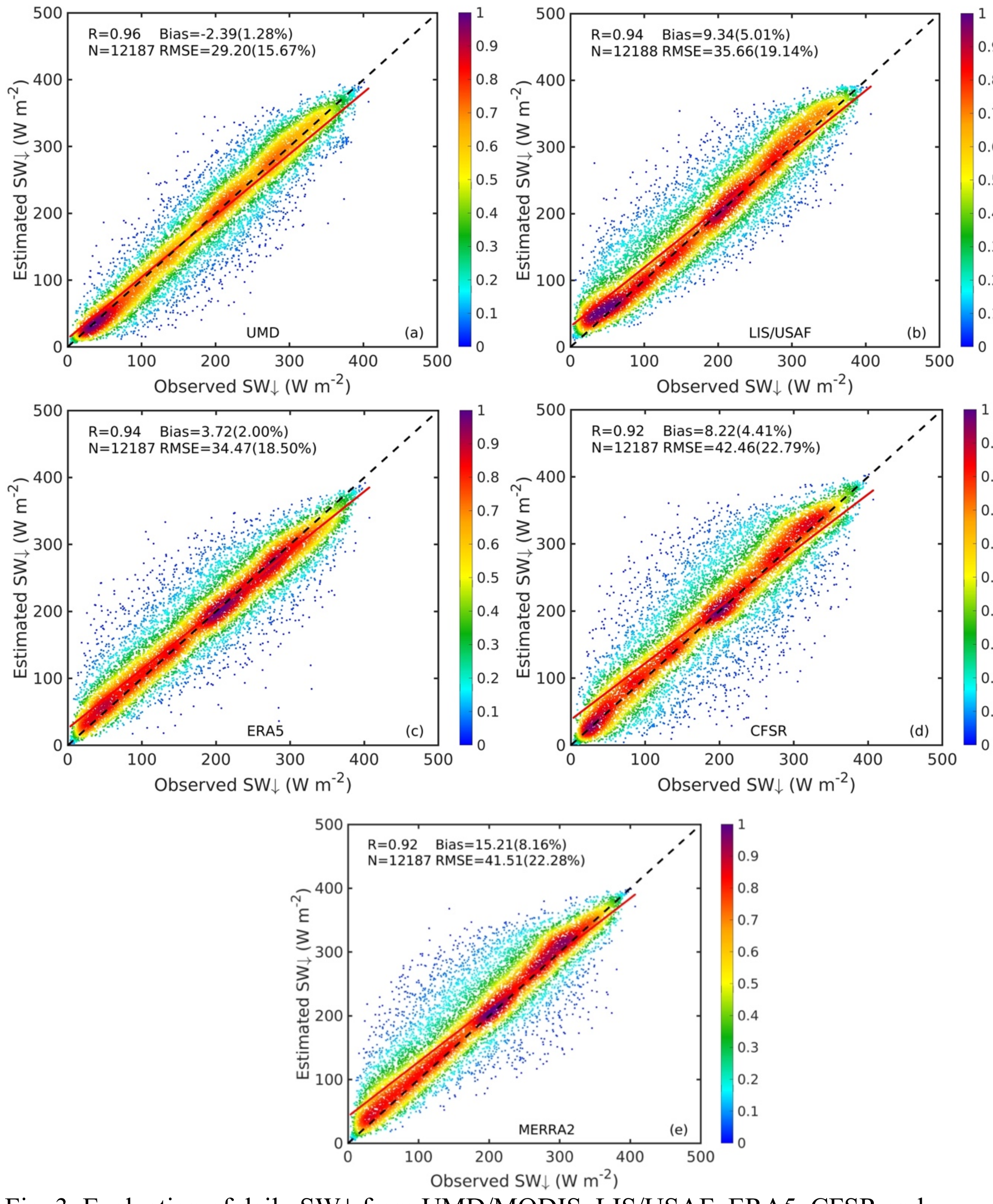

Fig. 3. Evaluation of daily SW↓ from UMD/MODIS, LIS/USAF, ERA5, CFSR and MERRA-2 against ground observations (all available sites) during the period of 10/01/2013 – 08/31/2015.

Table 2. Statistics of evaluation of daily SW↓ from UMD/MODIS, LIS3, ERA5, CFSR and MERRA-2 against ground observations 10/01/2013 – 08/31/2015. Units: W m^{-2}

	R	*Bias*	*(%)*	*RMSE*	*(%)*	*N*
UMD	0.96	-2.39	1.28	29.20	15.67	12187
LIS/USAF	0.94	9.34	5.01	35.66	19.14	12188
ERA5	0.94	3.72	2.00	34.47	18.50	12187
CFSR	0.92	8.22	4.41	42.46	22.79	12187
MERRA2	0.92	15.21	8.16	41.51	22.28	12187

2) EVALUATION OVER THE U.S.

Observations from seven BSRN sites and one ARM/SGPC1 site are used for comparisons. The BSRN stations are, "Desert_Rock_NV" (DRA, 36.63°N, 116.02°W), "Penn_State_PA"(PSU ,40.72°N, 77.93°W), "Bondville_IL" (BON, 40.06°N, 88.37°W), "Goodwin_Creek_MS" (GWN, 34.25°N, 89.97°W), "Fort_Peck_MT" (FPK, 48.31°N, 105.10°W), "Boulder_CO" (TBL, 40.13°N, 105.24°W), "Sioux_Falls_SD"' (SXF, 43.73°N, 96.62°W).

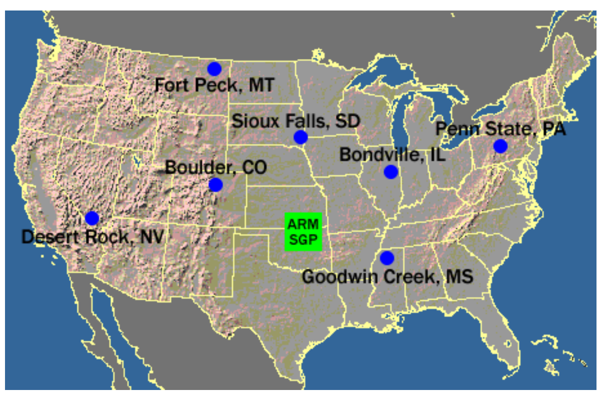

Fig. 4. SURFRAD sites and ARM/SGP location (Downloaded from SURFRAD website)

The site locations over the US are shown in **Figure 4**, results are shown in **Figure 5** and statistics are summarized in **Table 3**. As seen the UMD/MODIS product performs best with highest correlation *R of* (0.96), smallest *Bias* (-5.15 W m^{-2}) and *RMSE* (28.36 W m^{-2}). LIS/USAF product performs better than the other reanalysis products. The *R* of LIS/USAF is 0.94 with *Bias* of 10.63 W m^{-2} and *RMSE* of 35.51 W m^{-2}

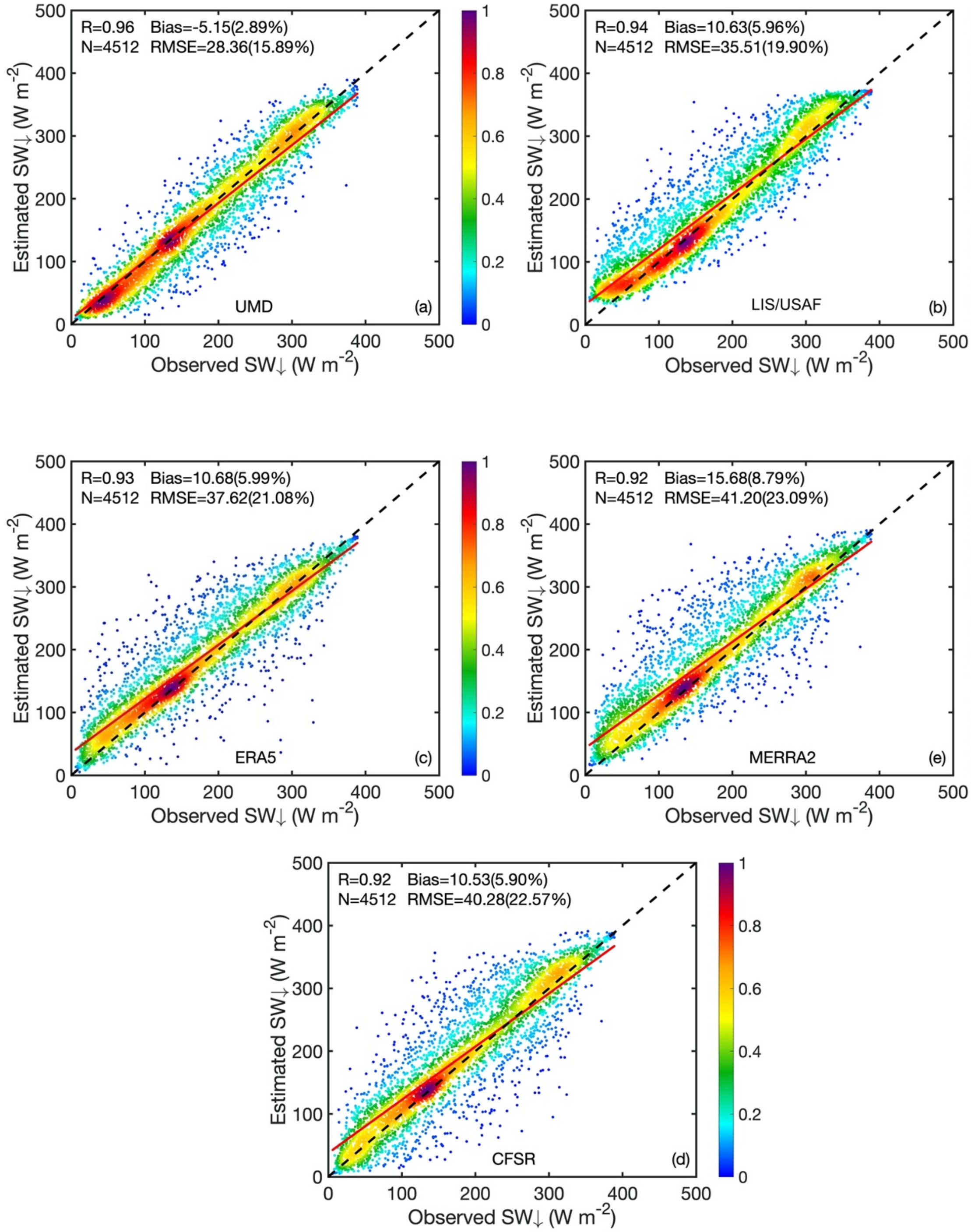

Fig. 5. Evaluation of daily SW↓ from UMD/MODIS, LIS/USAF, ERA5, CFSR and MERRA-2 against ground observations over U.S (7 SURFRAD sites and 1 ARM/SGPC1) during 10/01/2013 – 08/31/2015.

Table 3. Statistics of evaluation of daily SW↓ from UMD/MODIS, LIS/USAF, ERA5, CFSR and MERRA-2 against ground observations over U.S. during 10/01/2013 – 08/31/2015.

	R	***Bias***	***(%)***	***RMSE***	***(%)***	***N***
UMD	0.96	-5.15	2.89	28.36	15.89	4512
LIS/USAF	0.94	10.63	5.96	35.51	19.9	4512
ERA5	0.93	10.68	5.99	37.62	21.08	4512
CFSR	0.92	10.53	5.90	40.28	22.57	4512
MERRA2	0.92	15.68	8.79	41.20	23.09	4512

3) EVALUATION OVER EUROPE

Nine BSRN sites have been used for the Europe area. The locations of these sites are shown in **Figure 6**. The evaluations of the daily SW↓ from UMD/MODIS, LIS/USAF, ERA5, CFSR and MERRA-2 was conducted against the merged data of the nine sties for the study period as shown in **Figure 7**. The LIS/USAF product still performed better than the others. The *R* is 0.93, the *Bias* is 6.06 W m^{-2}, and *RMSE* is 35.93 W m^{-2}. The performance of CFSR and MERRA2 are comparable to each other.

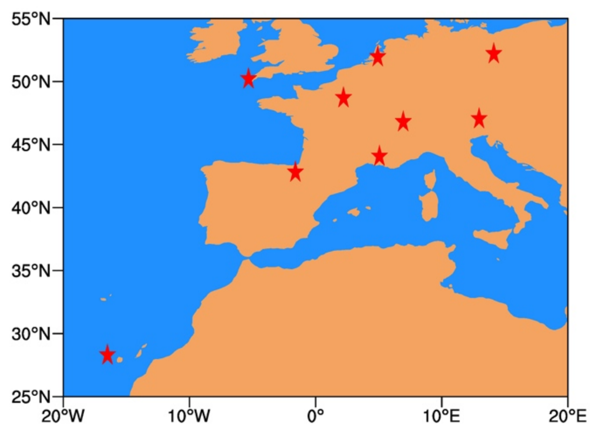

Fig. 6. Locations of 9 BSRN sites in Europe.

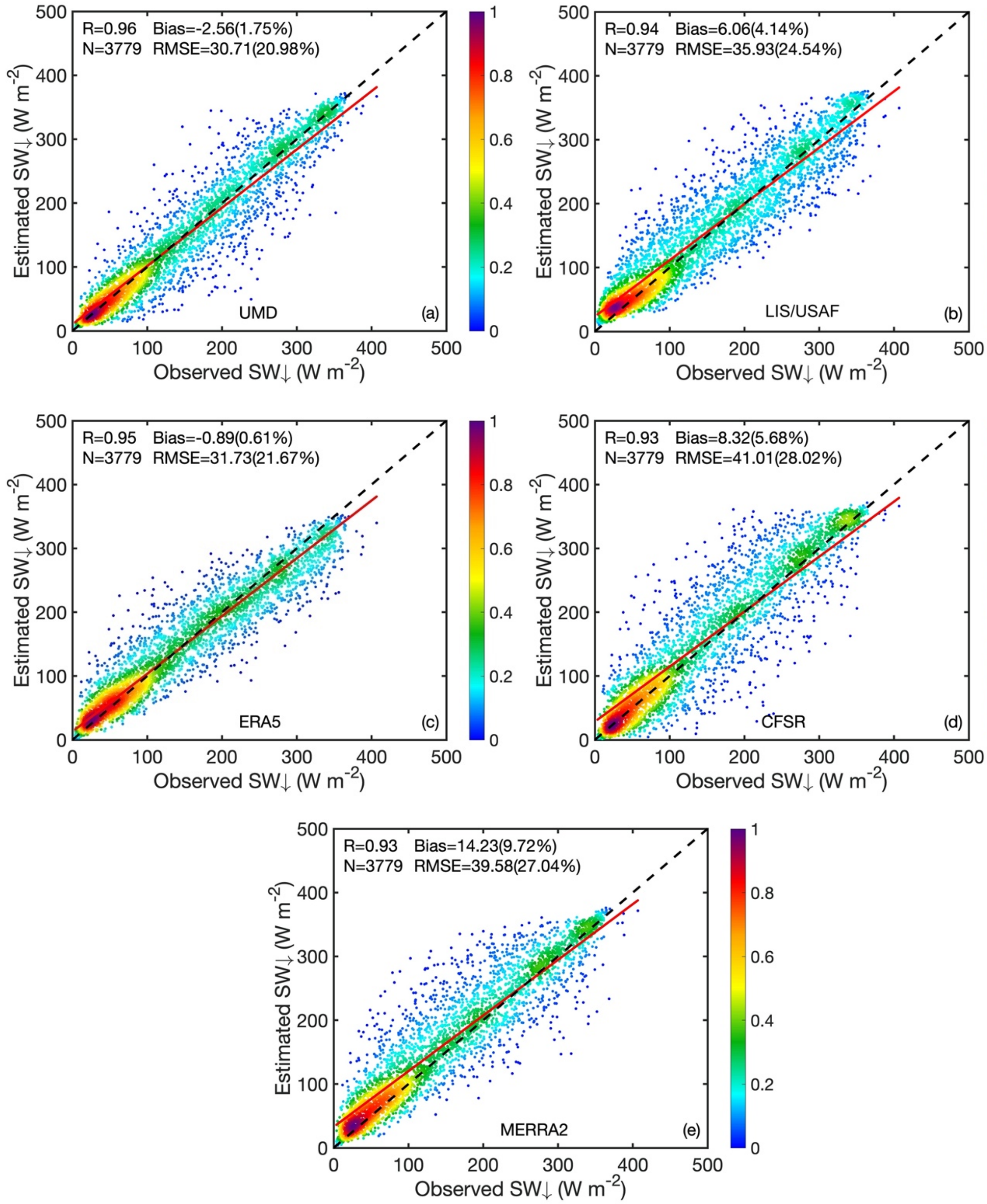

Fig.7. Evaluation of daily SW↓ from UMD/MODIS, LIS/USAF, ERA5, CFSR and MERRA-2 against ground observations over Europe during 10/01/2013 – 08/31/2015.

Table 4. Statistics of evaluation of daily SW↓ from UMD/MODIS, LIS3, ERA5, CFSR and MERRA2 against ground observations over Europe during 10/01/2013 – 08/31/2015.

	R	*Bias*	*(%)*	*RMSE*	*(%)*	*N*
UMD	0.96	-2.56	1.75	30.71	20.98	3779
LIS3	0.94	6.06	4.14	35.93	24.54	3779
ERA5	0.95	-0.89	0.61	31.73	21.67	3779
CFSR	0.93	8.32	5.68	40.01	28.02	3779
MERRA2	0.93	14.23	9.72	39.58	27.04	3779

d. Comparison of LIS/USAF SW↓ with independent products at global scale

8. EVALUATION OVER the GLOBE

The averaged SW↓ from LIS/USAF WWMCA, ERA5, CFSR, MERRA-2 for January during 10/01/2013-08/31/2015 were compared against UMD/MODIS. As shown in **Figures 8-9**, the distribution pattern and the averaged values of the SW↓ for January are similar in North America, Europe and Australia. Differences are noted mainly in South America, Africa and Asia. **Figure 10** shows the frequency distribution of these differences. The reanalysis products tend to overestimate the SW↓ fluxes when compared to satellite observation for January, and most of the differences are less than 20 W m^{-2}. Statistics are shown in **Table 5**. The correlation coefficients (*R*) between the reanalysis products and satellite observation are over 0.9 with positive *Bias* (≤15.1 W $m^{-2.}$). The root mean-square errors (*RMSE*) are in the range of 31.8~43.9 W $m^{-2.}$

Used is the Student's t-test to test the null hypothesis that the sample means are from the same population (i.e. H0: ave1=ave2). **p** is the significance which is two tailed and uses the incomplete beta function to calculate the probability. It will range between zero and one. If p less than significance level, then the null hypothesis is rejected and the alternative hypothesis is accepted. In our case, we assume that UMD/MODIS has the same average values as the LIS/USAF or ERA5 or CFSR or MERRA2 and the significance level is 0.1.

All the **p** values are equal or larger than 0.1. Therefore, we can assume that the samples are similar to each other.

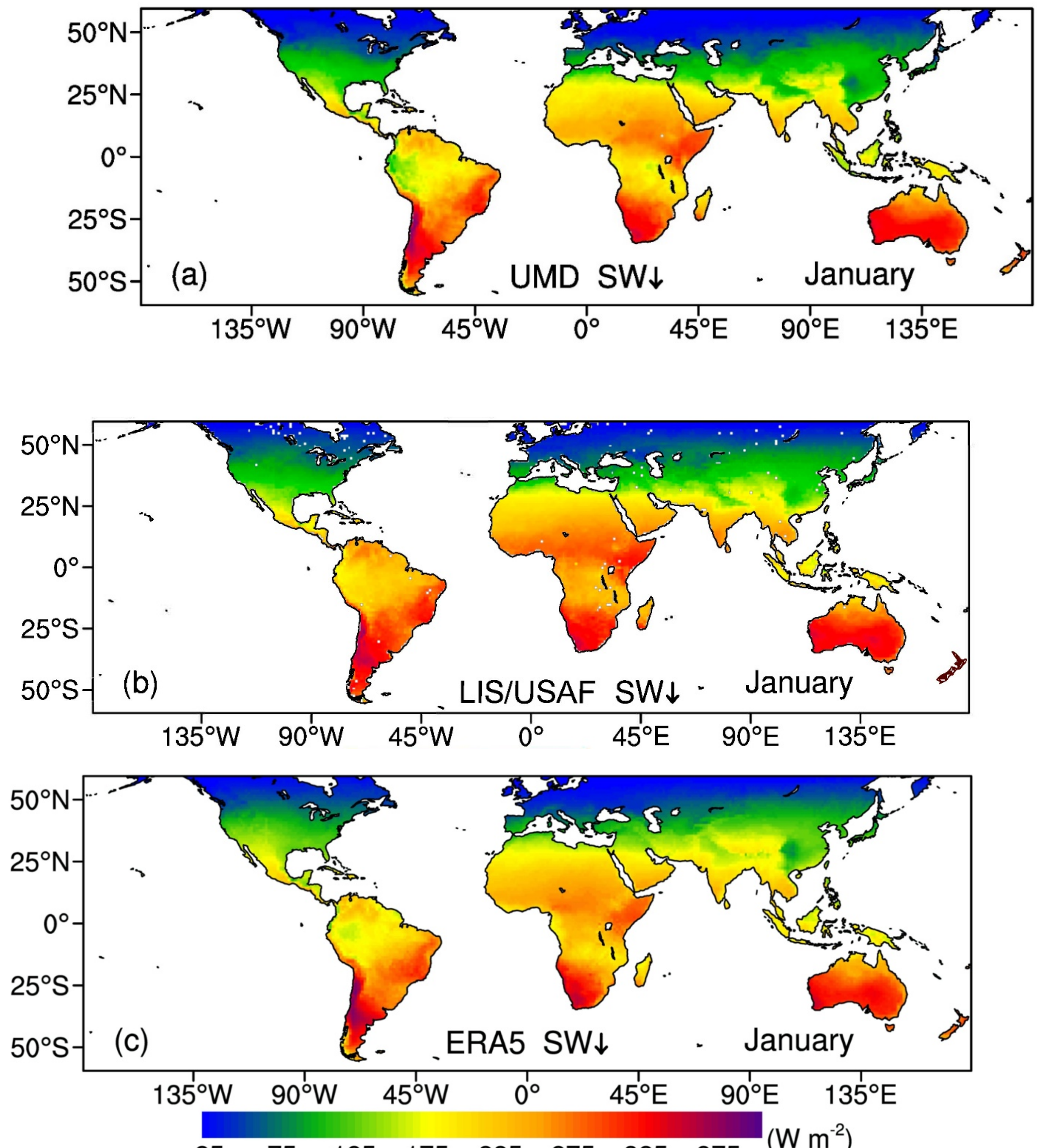
50°N
25°N
0°
25°S
50°S
(a)
UMD SW↓
January
135°W
90°W
45°W
0°
45°E
90°E
135°E
(b)
LIS/USAF SW↓
January
(c)
ERA5 SW↓
January
25
75
125
175
225
275
325
375
(W m-2)

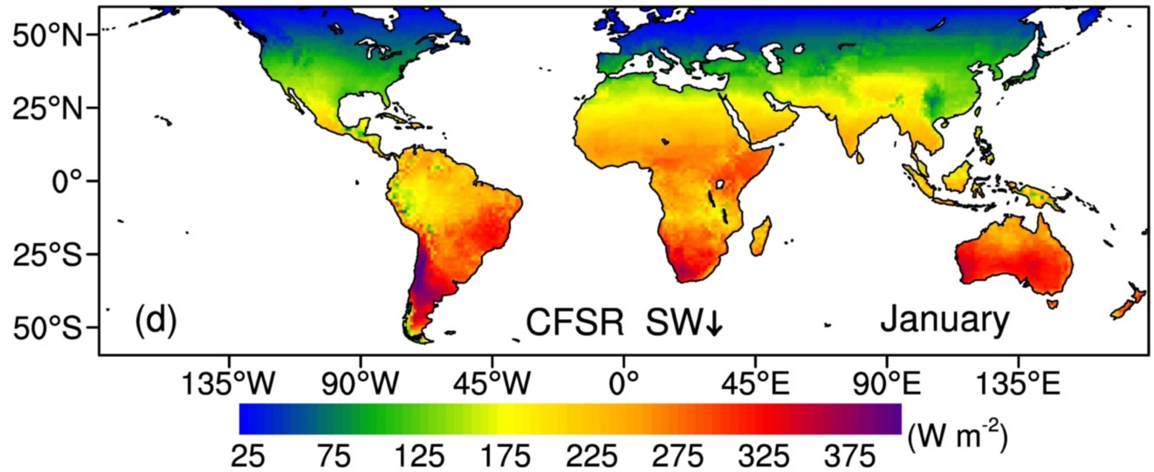

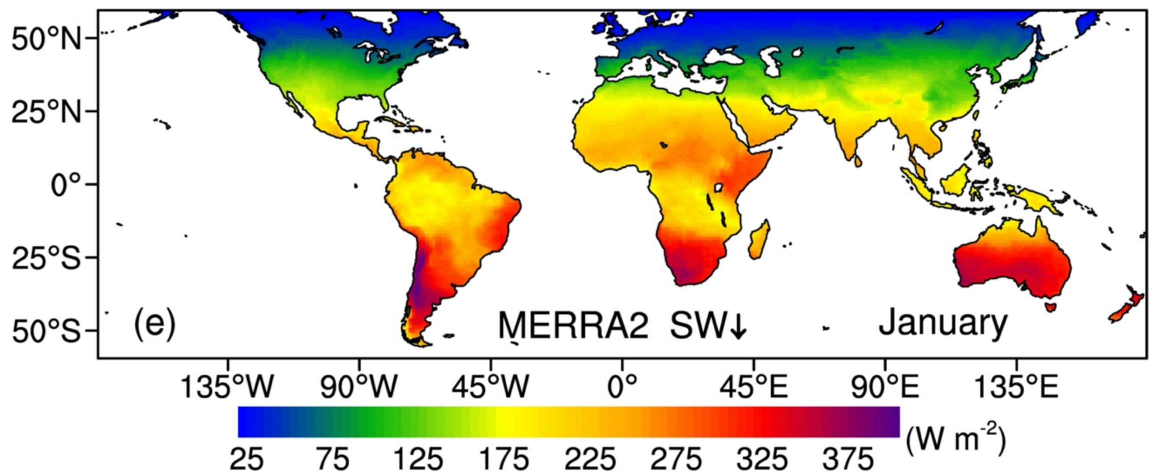

Fig. 8. Averaged daily SW↓ from LIS/USAF, ERA5, CFSR, MERRA-2 and UMD/MODIS for January during 10/01/2013-08/31/2015.

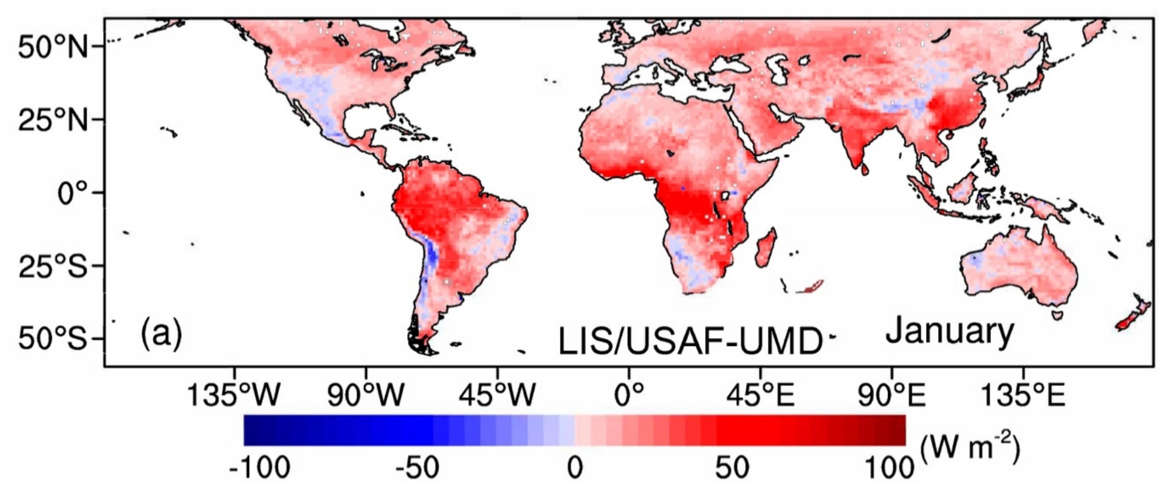

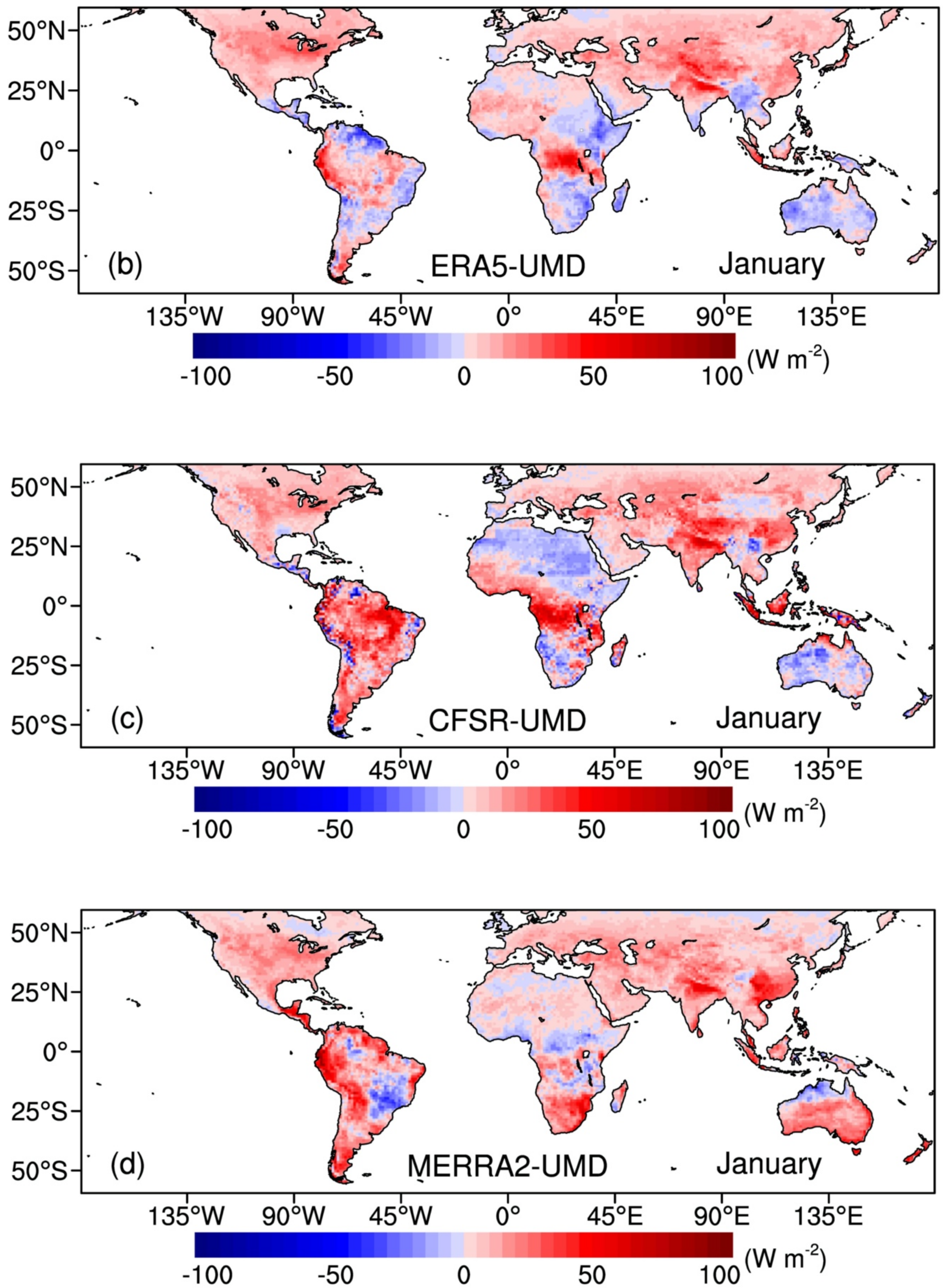

Fig. 9. Averaged daily SW ↓ difference between LIS/USAF, ERA5, CFSR, MERRA-2 and UMD/MODIS for January during 10/01/2013-08/31/2015.

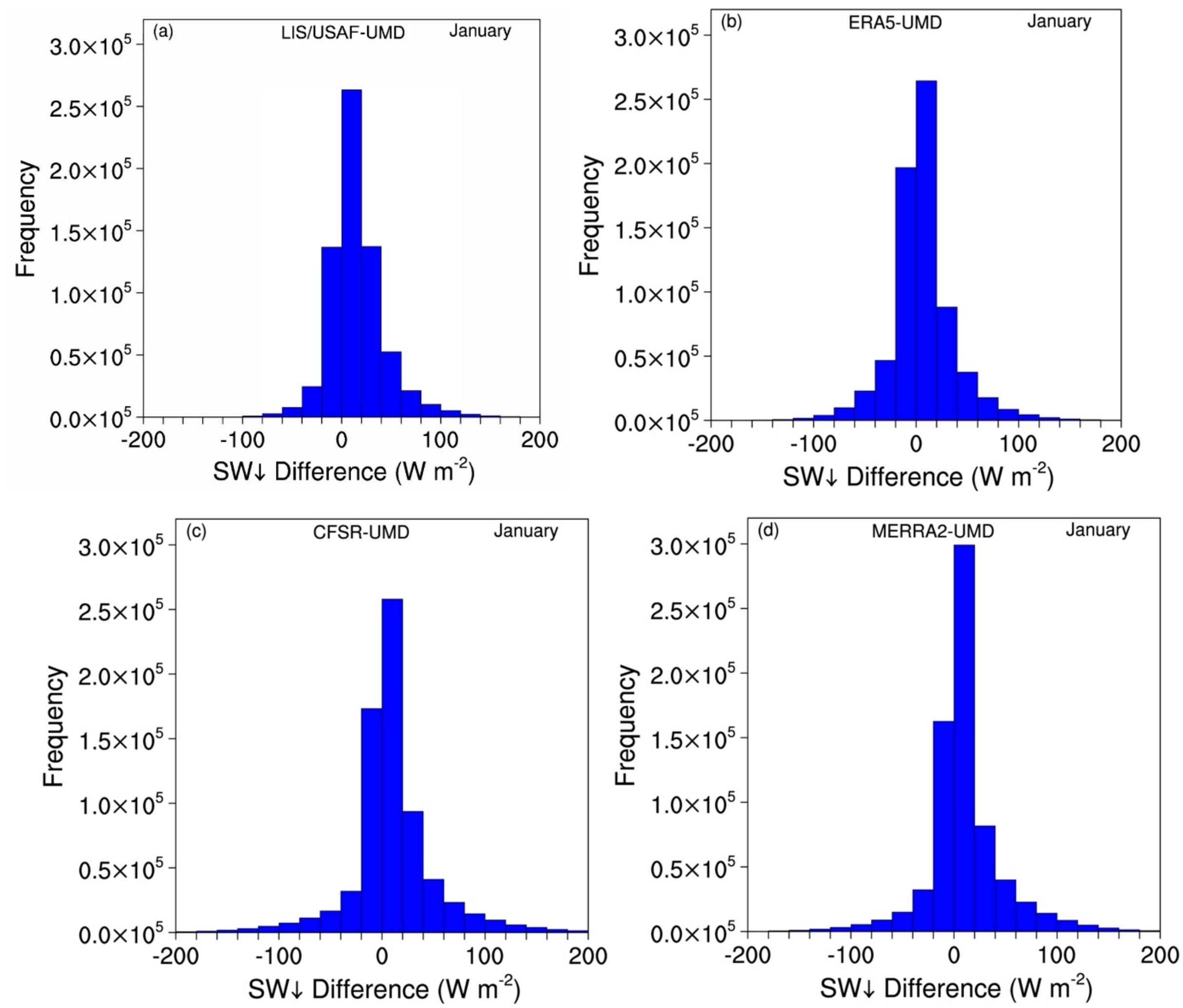

Fig.10. Distribution of daily SW ↓ difference between LIS/USAF, ERA5, CFSR, MERRA2 and UMD/MODIS for January during 10/01/2013-08/31/2015

The averaged SW↓ from LIS/USAF, ERA5, CFSR, MERRA-2 for July over the study period were also compared against UMD/MODIS and their differences are shown in **Figure 11.** The re-analysis products of LIS/USAF, CFSR and MERRA-2 tend to overestimate the SW↓ fluxes for July when compared with the UMD/MODIS product, especially in Asia. The frequency distribution of the differences (**Figure 12)** also shows such tendency except for ERA5. Most of the differences are within $\pm$20 W m^{-2}. The correlation coefficients between the reanalysis and satellite observation are over 0.8. All of the reanalysis products have positive bias ($\leq$35.0 W $m^{-2.}$) and the *RMSE*s are in between 41.6~59.7 W m^{-2}.

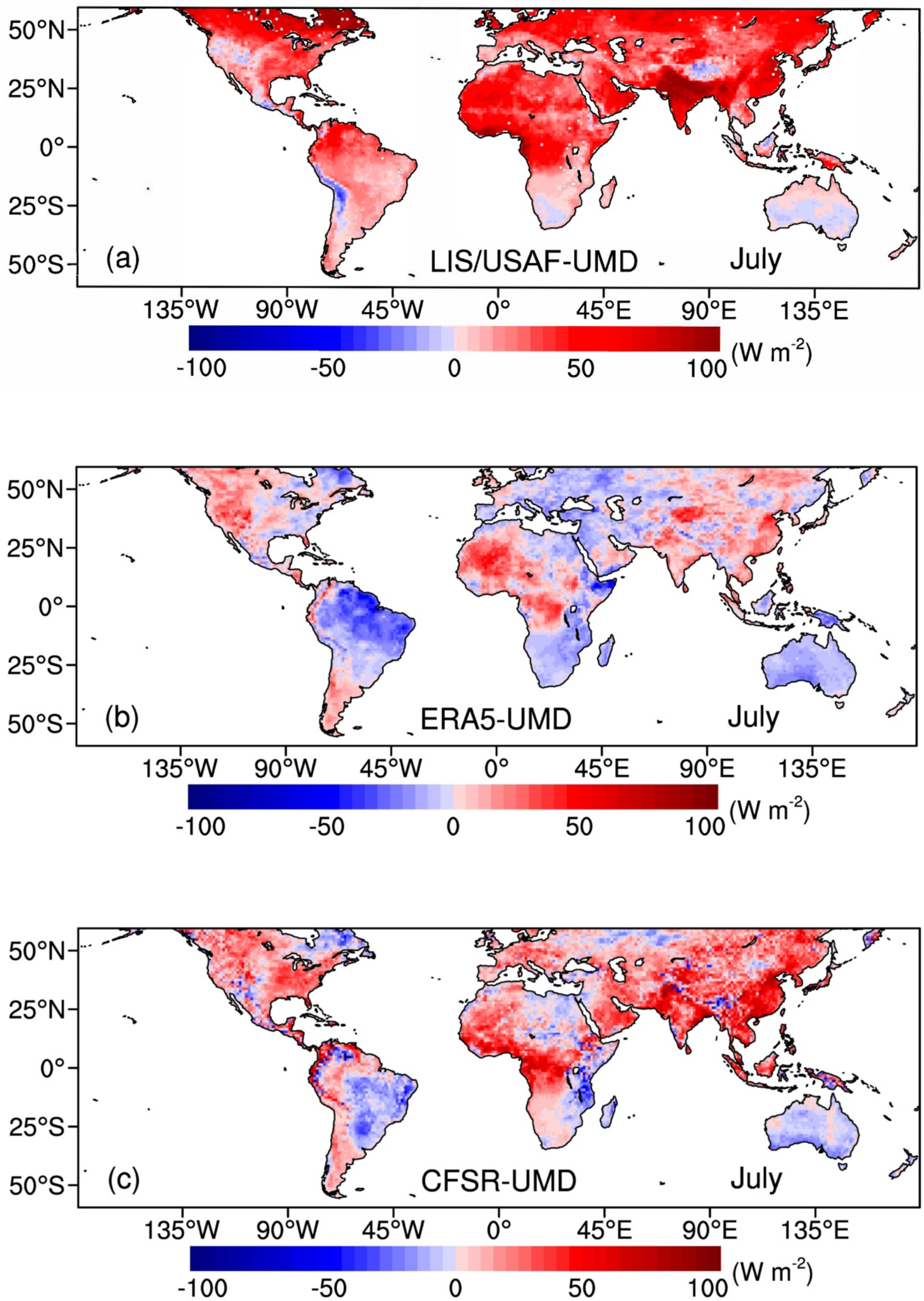
(a)
LIS/USAF-UMD
July
(b)
ERA5-UMD
July
(c)
CFSR-UMD
July
50°N
25°N
0°
25°S
50°S
135°W
90°W
45°W
0°
45°E
90°E
135°E
-100
-50
0
50
100
(W m-2)

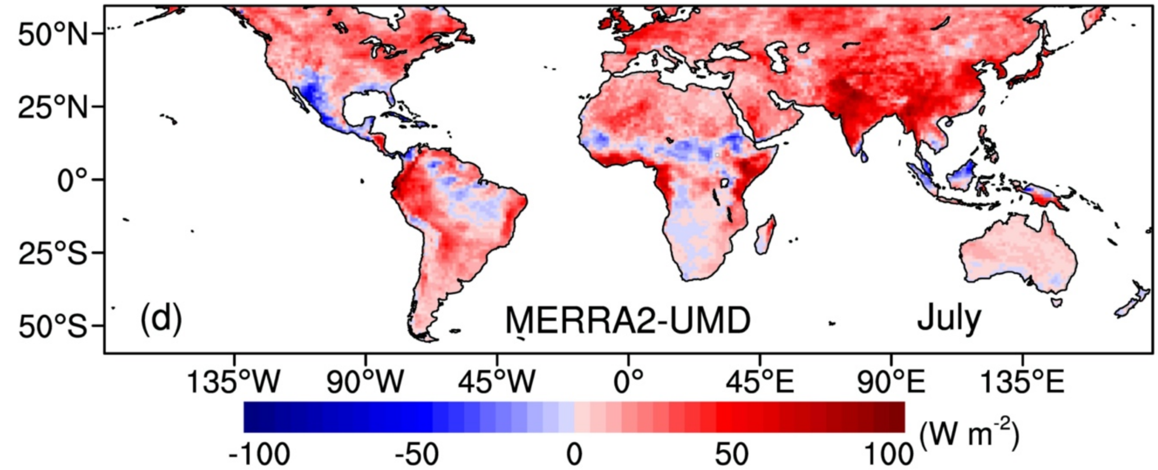

Fig. 11. Averaged daily SW ↓ difference between LIS/USAF, ERA5, CFSR, MERRA-2 and UMD/MODIS for July during 10/01/2013~08/31/2015.

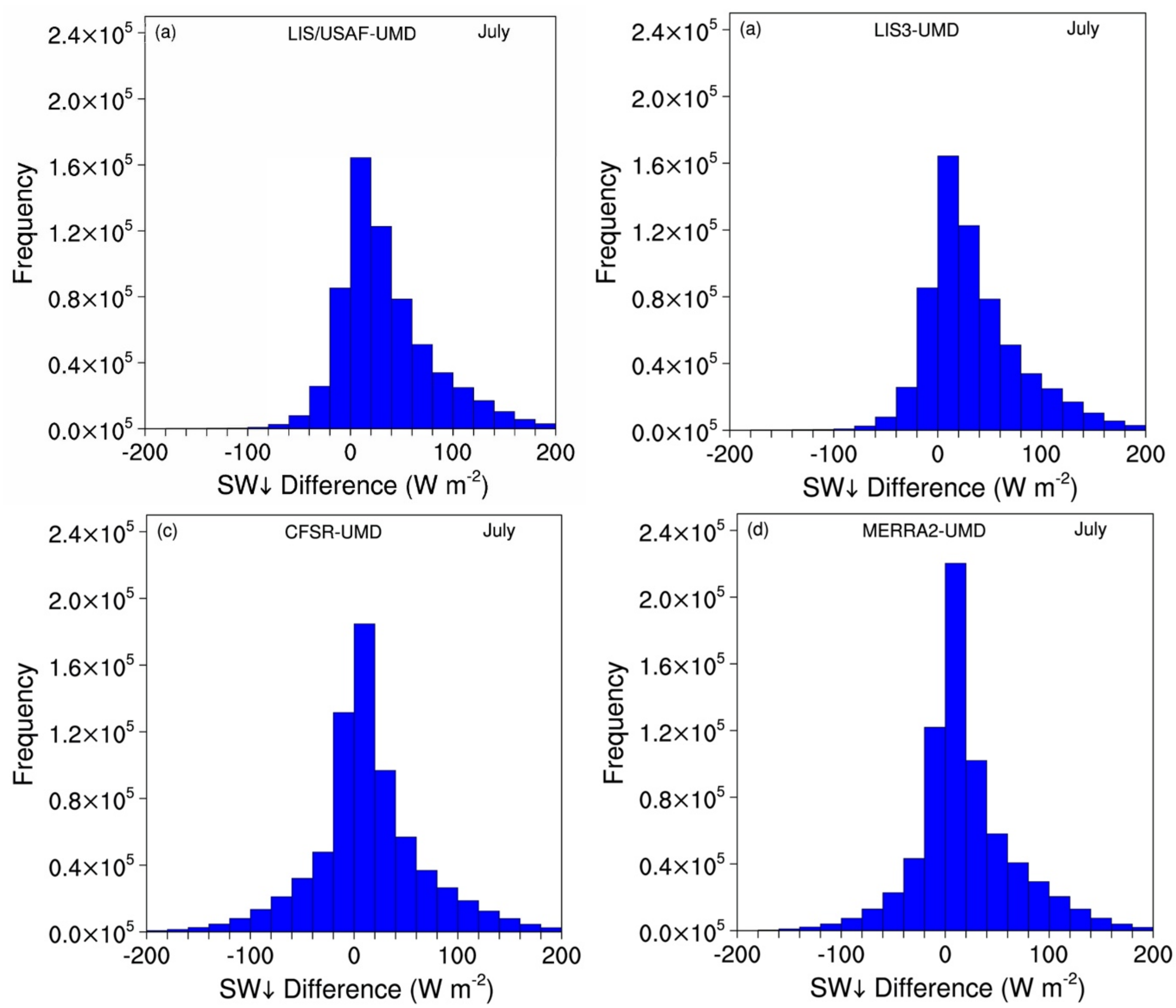

Fig. 12. Distribution of daily SW↓ difference between ERA5, CFSR, MERRA-2, LIS/USAF and UMD/MODIS for July during 10/01/2013~08/31/2015.

Table 5. Statistics of evaluations of daily SW↓ for January and July against UMD/MODIS for the entire study area from 10/01/2013~08/31/2015. Here ***p*** is the significance.

	January						**July**					
UMD	*R*	***Bias***	*%*	***RMSE***	*%*	***p***	***R***	***Bias***	*%*	***RMSE***	*%*	***p***
LIS3	0.96	15.1	9.8	31.8	20.7	0.2	0.83	35.0	15.2	59.7	25.9	0.1
ERA5	0.96	6.4	4.2	30.9	20.1	0.3	0.88	0.7	0.3	40.6	17.6	0.3
CFSR	0.92	10.1	6.6	43.9	28.6	0.2	0.81	13.6	5.9	56.1	24.3	0.2
MERRA2	0.94	10.2	6.6	38.3	25.0	0.2	0.83	19.1	8.3	51.6	22.4	0.2

6. Discussion and Summary

As stated in Kumar et al. (2006) land surface modeling seeks to predict the terrestrial water, energy, and biogeochemical processes by solving the governing equations at the earth/atmosphere interface. LSMs typically require several types of inputs states such as states known as ''forcing'' such as information on clouds. Using these inputs, LSMs can predict surface fluxes providing a realistic representation of the transfer of mass, energy, and momentum between a vegetated surface and the atmosphere. One of the important boundary conditions to the LSMs is SW↓ radiation. From the global scale comparisons, it became evident that most models have problems to predict this parameter correctly in certain climatic regions and models differ seasonally. For instance, during January, USAF shows overestimates primarily over S. America, equatorial Africa, India and China and underestimation over North Africa. CFSR also shows overestimates over India and China, equatorial Africa but underestimates over North Africa. ERA5 overestimates over the Himalayas and sub-equatorial Africa but differences with UMD/MODIS are much smaller than those seen in LIS/USAF. MERRA2 also tends to over-estimate over the Himalayas and China but shows a mixture of over-estimation and under-estimation over S. America. Notable differences between the models are seen over Australia. In July, there seems to be a systematic overestimation by LIS/USAF over most of the globe while the other models alternate between over-estimation and under-estimation. It should be noted that as yet, there is no full agreement between available estimates of cloud amounts (Wonsick et al., 2009). Some inference schemes to derive surface radiative fluxes use information on cloud optical depth rather than on cloud amount but again, the methodologies how to derive such information from satellite observations differ (Wang and Pinker, 2008; Platnick et al. 2017)

Another accuracy issue in SW↓ fluxes as derived from satellite observations is related to the nonlinearity of the relationship between radiance and flux. In most cases, provided are radiances averaged at a certain scale and these are used to compute the flux. An example that illustrates this issue is the International Satellite Cloud Climatology Project (ISCCP) product (Rossow and Schiffer 1991) that is widely used to produce surface fluxes. For instance, what is known as the ISCCP D1 product provides spectral SW radiances at the top of the atmosphere at 2.5^{o} spatial resolution. There exists also what is known as the ISCCP DX product which is sampled at 30 km. An experiment was conducted (Ma and Pinker, 2012) to compute the SW↓ from ISCCP D1 and from ISCCP DX (which was first aggregated to 0.5^{o} resolution). When the 0.5^{o} product was upscaled to 2.5^{o} and compared to the 2.5^{o} derived directly from the ISCCP D1 product, differences were found when compared to ground observations. The 0.5^{o} product upscaled to 1^{o} had a bias of -0.5 Wm^{-2} while the one from the ISCCP D1 had a bias of 5.7 Wm^{-2}.

The MODIS products are also available at about 5 km resolution. Based on the findings reported in Ma and Pinker (2009) it is hypothesized that if the SW↓ fluxes were to be produced at that scale and upscaled to any of the resolutions used in comparison, the agreement with ground observations would improve. Another potential of improvement is to better represent the diurnal cycle of the MODIS SW↓ products. This study is a first attempt of its kind to obtain a comprehensive evaluation of the LIS/USAF SW↓ fluxes. It was shown that overall, at global scale the LIS USAF model tends to overestimate the surface SW↓ fluxes. It was also learned that compared to major re-analyses products over different climatic regions the LIS/USAF model performed frequently better than several of the reanalysis products when evaluated against satellite and ground observations.

Acknowledgment

This work was supported under Grant number 80NSSC20K0656 from NASA/GSFC to the University of Maryland. The work benefited from support under NASA grant NNX08AN40A from the Science Mission Directorate-Division of Earth Science and NASA grant NNX13AC12G, the Energy and Water Cycle Study (NEWS) program to the University of Maryland. Thanks are due to the NASA Goddard Earth Sciences Data and Information Services Center, which developed and maintains the Giovanni online data system that was used to obtain and manipulate the MODIS data; to the various MODIS teams that produced the data that were used in this study. We acknowledge the ECMWF for providing the ERA5 data; the MERRA-2 data are provided by the Global Modeling and Assimilation Office (GMAO), NASA/GSFC; and NCEP Reanalysis data are provided by the NOAA/OAR/ESRL PSD, Boulder, Colorado, USA. The BSRN/SURFRAD data are provided by the NOAA Earth System Research Laboratory, Global Monitoring Division (https://www.esrl.noaa.gov/gmd/grad/surfrad/).

Data Availability Statement

https://bsrn.awi.de/

https://www.arm.gov/capabilities/observatories/sgp

https://climatedataguide.ucar.edu/climate-data/climate-forecast-system-reanalysis-cfsr

https://earthdata.nasa.gov/"

https://gmao.gsfc.nasa.gov/reanalysis/MERRA-2/data_access/

https://cds.climate.copernicus.eu/cdsapp#!/dataset/reanalysis-era5-single-levels?tab=overview

Shortwave flux estimates from MODIS: Upon Request.

References

Aires, F., C. Prigent, and W. B. Rossow, 2004: Temporal interpolation of global surface skin temperature diurnal cycle over land under clear and cloudy conditions. *J. Geophys*. Res*.,* **109,** D04313, doi: 10.1029/2003JD003527

Arsenault, K., S Kumar, J. Geiger, S. Wang, E. Kemp, D. Mocko, H Beaudoing, A. Getirana, M. Navari, B. Li, J. Jacob, J. Wegiel, and C. Peters-Lidard, 2018: The Land surface Data Toolkit (LDT v7.2) – a data fusion environment for land data assimilation systems. *Geosci. Model Dev.,* **11**, 3605-3621, https://doi.org/10.5194/gmd-11-3605-2018.

Augustine, J., J. DeLuisi C. Long, 2000: Surfrad e a national surface radiation budget network for atmospheric research. *Bulletin of the American Meteorological Society,* **81** (10), 2341e2358.

Augustine, J.A., G. B. Hodges, C. R. Cornwall, J. J. Michalsky, and C. I. Medina, 2005: An update on SURFRAD: The GCOS surface radiation budget network for the continental United States. *J. Atmos. Oceanic Technol.*, **22**, 1460-1472, DOI 10.1175/JTECH1806.1.

Augustine, J. A., and E. G. Dutton, 2013: Variability of the surface radiation budget over the United States from 1996 through 2011 from high-quality measurements. *Journal of Geophysical Research: Atmospheres,* **118,** 43–53, https://doi.org/10.1029/2012JD018551

Chou, M.-D., and M. J. Suarez, 1999: A solar radiation parameterization for atmospheric studies. *NASA Tech. Memo*. NASA/TM-1999-104606, 38 pp. [Available online at http://ntrs.nasa.gov/archive/nasa/casi.ntrs.nasa.gov/19990060930.pdf.]

——, K.-T. Lee, and P. Yang, 2002: Parameterization of shortwave cloud optical properties for a mixture of ice particle habits for use in atmospheric models. *J. Geophys. Res*., **107**, 4600, doi:10.1029/2002JD002061.

Dai, Y., X. Zeng., R. Dickinson, I. Baker, G. Bonan, M. Bosilovich, S. Denning, P. Dirmeyer, P. Houser, G. Niu, K. Oleson, A. Schlosser, and Z.-L. Yang, 2003: The Common Land Model. *Bulletin of The American Meteorological Society*, ***84***, 1013-1023. doi:10.1175/BAMS-84-8-1013.

D'Entremont, R. P., R. Lynch, G. Uymin, J.-L. Moncet, R. B. Aschbrenner, M. Conner, and G. B. Gustafson, 2016: Application of Optimal Spectral Sampling for a Real-Time Global Cloud Analysis Model. *Weather and Forecasting*, **31**, 743- 761.

Dickenson, R. E., A. Henderson-Sellers, P. J. Kennedy, 1993: Biosphere–Atmosphere Transfer Scheme (BATS) version 1E as coupled to the NCAR Community Climate Model. *Tech. Note NCAR/TN-387+STR*, 72 pp. [Available from NCAR, P.O. Box 3000, Boulder, CO 80307.].

Driemel, A., J. Augustine, K. Behrens, S. Colle, C. Cox, E. Cuevas-Agulló, F. M. Denn, T. Duprat, M. Fukuda,, H. Grobe, M/ Haeffelin, Hodges, G., Hyett, N., Ijima, O., Kallis, A., Knap, W., Kustov, V., Long, C. N., Longenecker, D., Lupi, A., Maturilli, M., Mimouni, M., Ntsangwane, L., Ogihara, H., Olano, X., Olefs, M., Omori, M., Passamani, L., Pereira, E. B., Schmithüsen, H., Schumacher, S., Sieger, R., Tamlyn, J., Vogt, R., Vuilleumier, L., Xia, X., Ohmura, A., andG. König-Langlo, 2018: Baseline Surface Radiation Network (BSRN): structure and data description (1992–2017). *Earth Syst. Sci. Data*, **10,** 1491–1501, https://doi.org/10.5194/essd-10-1491-2018.

Ek, M., Mitchell, K., Yin, L., Rogers, P., Grunmann, P., Koren, V., Gayno, G., Tarpley, J., 2003: Implementation of Noah landsurface model advances in the NCEP operational mesoscale Eta model. *Journal of Geophysical Research,* **108** (D22), doi:10.1029/ 2002JD003296.

Gelaro, R., W. McCarty, M. J. Suárez, R. Todling, A. Molod, L. Takacs, C. A. Randles, A. Darmenov, M. G. Bosilovich, R. Reichle, et al., 2017: The Modern-Era Retrospective Analysis for Research and Applications, Version 2 (MERRA-2). *J. Clim.*, **30**, 5419–5454.

Hansen, M., R. DeFries, J. Townshend, R. Sohlberg, 2000: Global land cover classification at 1km spatial resolution using a classification tree approach. *International Journal of Remote Sensing,* **21** (6), 1331e1364

Hersbach, H., P. de Rosnay, B. Bell, D. Schepers, A. Simmons, C. Soci, S. Abdalla, et al., 2018: Operational Global Reanalysis: Progress, Future Directions and Synergies with NWP. *ERA Report Series. Document,* **27**, 12/2018. https://www.ecmwf.int/node/18765.

Kleist, D. T., D. F. Parrish, J. C. Derber, R. Treadon, W.-S. Wu, and S. Lord, 2009. Introduction of the GSI into the NCEPs Global Data Assimilation System. Wea. Forecasting, 24, 1691–1705, doi: 10.1175/2009WAF2222201.1.

Kumar, S V, C. D. Peters-Lidard, Y. Tian, P. R. Houser, J. Geiger, S. Olden, L. Lighty, J. L. Eastman, B. Doty, P. Dirmeyer, J. Adams, K. Mitchell, E. F. Wood and J. Sheffield, 2006: Land Information System - An interoperable framework for high resolution land surface modeling. *Environmental Modelling & Software,* **21**, 1402-1415.

Kumar, S. V., C. D. Peters-Lidard, Y. Tian, R. H. Reichle, J. Geiger, C. Alonge, J. Eylander, and P. Houser, 2008a: An integrated hydrologic modeling and data assimilation framework enabled by the Land Information System (LIS). *IEEE Computer*, **41**, 52-59, doi:10.1109/MC.2008.475.

Kumar, S. V., R. H. Reichle, C. D. Peters-Lidard, R. D. Koster, X. Zhan, W. T. Crow, J. B. Eylander and, P R. Houser, 2008: A land surface data assimilation framework using the Land Information System: Description and applications, *Advances in Water Resources,* **31**, 1419-1432.

Kumar, S V, C D Peters-Lidard, D M Mocko, and Y Tian, 2013: Multiscale evaluation of the improvements in surface snow simulation through terrain adjustments to radiation. *Journal of Hydrometeorology*, **14**, 220-232, doi: http://dx.doi.org/10.1175/JHM-D-12-046.1.

NASA LIS Website: http://lis.gsfc.nasa.gov/.

Ma, Y. and R. T. Pinker, 2012. Shortwave Radiative Fluxes from Satellites: An Update. *J. Geophys. Res. Atmos.,* **117**, Issue D23, DOI: 10.1029/2012JD018332.

Mitchell, K.E., Lohmann, D., Houser, P.R., Wood, E.F., Schaake, J.C., Robock, A., Cosgrove, B., Sheffield, J., Duan, Q., Luo, L., Higgins, W.R., Pinker, R.T., Tarpley, J.D., Lettenmaier, D.P., Marshall, C.H., Entin, J.K., Pan, M., Shi, W., Koren, V., Meng, J., Ramsay, B.H., Bailey, A.A., 2004: The Multi-institution North American Land Data Assimilation system (NLDAS): utilization of multiple GCIP products and partners in a continental distributed hydrological modeling system. *Journal of Geophysical Research,* **109**, doi:10.1029/2003JD003823.

Molod, A., L. Takacs, M. Suárez, and J. Bacmeister, 2015: Development of the GEOS-5 atmospheric general circulation model: Evolution from MERRA to MERRA2. Geosci. Model Dev., 8, 1339–1356, doi:10.5194/gmd-8-1339-2015.

Niu, X. and R. T. Pinker, 2015: An improved methodology for deriving high resolution surface shortwave radiative fluxes from MODIS in the Arctic region. *J. Geophys. Res.* Atmos., **120**, 2382–2393, doi: 10.1002/2014JD022151.

Ohmura, A., E. G. Dutton, B. Forgan, Fröhlich, H. Gilgen, H. Hegner, A. Heimo, G. König-Langlo, B. McArthur, G. Müller, G., et al., 1988: Baseline Surface Radiation Network (BSRN/WCRP): New precision radiometry for climate research. *Bull. Am. Meteorol. Soc*., **79,** 2115–2136. 42.

Pinker, R. T., D. Sun, M. Miller, and G. Robinson, 2007: Diurnal cycle of land surface temperature in a desert encroachment zone as observed from satellites. *Geophys. Res. Lett.,* **34** Issue: 11 Article Number: L11809.

Pinker, R. T., X. Li, W. Meng, et al., 2007: Toward improved satellite estimates of short-wave radiative fluxes - Focus on cloud detection over snow: 2. Results. *JGR-Atmospheres*, **112** Issue: D9 Article Number: D09204.

Pinker, R. T., B. Z. Zhang, R. A. Weller, and, W. Chen, 2018: Evaluating surface radiation fluxes observed from satellites in the southeastern Pacific Ocean. *Geophysical Research Letters,* **45**, https://doi.org/10.1002/2017GL076805.

Platnick, S., et al., 2017: The MODIS Cloud Optical and Microphysical Products: Collection 6 Updates and Examples from Terra and Aqua. *IEEE Trans. Geosci. Remote Sens*., **55**, 502-525, doi:10.1109/TGRS.2016.2610522.

Putman, W., and S.-J. Lin, 2007: Finite-volume transport on various cubed-sphere grids. J. Comput. Phys., 227, 55–78, doi: 10.1016/j.jcp.2007.07.022.

Ramaswamy, V., and S. M. Freidenreich, 1992: A study of broadband parameterizations of the solar radiative interactions with water vapor and water drops. J. Geophys. Res., **97**, 11 48711 512, doi: 10.1029/92JD00932.

Randles, C. A., and Coauthors, 2013: Inter-comparison of shortwave radiative transfer schemes in global aerosol modeling: Results from the AeroCom Radiative Transfer Experiment. Atmos. Chem. Phys., **13**, 2347–2379, doi: 10.5194/acp-13-2347-2013.

Rienecker, M. M., and Coauthors, 2008: The GEOS-5 Data Assimilation System—Documentation of versions 5.0.1, 5.1.0, and 5.2.0. Technical Report Series on Global Modeling and Data Assimilation, Vol. 27, NASA Tech. Rep. NASA/TM-2008-104606, 118 pp.

Rodell, M., Houser, P. R., Jambor, U., Gottschalck, J., Mitchell, K., Meng, C.-J., Arsenault, K., Cosgrove, B., Radakovich, J., Bosilovich, M., Entin, J. K., Walker, J. P., D. Lohmann, D. Toll, 2004: The Global Land Data Assimilation System. Bulletin of the American Meteorological Society **85** (3), 381e394.

Rossow, W. B., and R. A. Schiffer 1999: Advances in understanding clouds from ISCCP. *Bull. Am. Meteorol. Soc*., **80**, 2261–2287, doi:10.1175/ 1520-0477(1999)0802.0.CO;2.

Saha, S., S. Moorthi, H.-L. Pan, X. Wu, J. Wang, S. Nadiga, P. Tripp, et al. 2010: The NCEP Climate Forecast System Reanalysis. *Bull. Amer. Meteorol. Soc.,* **91** (8): 1015–1058. doi: 10.1175/2010BAMS3001.1.

Saha S., S. Moorthi, X. Wu, J. Wang, S. Nadiga, P. Tripp, et al., 2014: The NCEP Climate Forecast System Version 2. *Journal of Climate*, **27** (6), 2185–2208, doi: 10.1175/JCLI-D-12-00823.1.

Sellers, P. J., Y. Mintz, A. Dalcher, 1986: A simple biosphere model (SiB) for use within general circulation models. *Journal of Atmospheric Science* **43**, 505e531.

Sellers, P. J., Y. Mintz, Y. C. Sud, and A. Dalcher, 1986: A simple biosphere model (SiB) for use within general circulation models. *J. Atmos. Sci.,* **43,** 505–531.

Stokes, G. M., and S. E. Schwartz, 1994: The Atmospheric Radiation Measurement (ARM) Program: Programmatic background and design of the Cloud and Radiation Testbed. *Bull. Amer. Meteorol. Soc.* **75**, 1201-1221.

Trenberth, K. E., D. P. Stepaniak, J. M. Caron, 2002: Accuracy of atmospheric energy budgets from analyses. *J. Clim*., **15**, 3343–3360.

Wang, H., R. T. Pinker, P. Minnis, and M. M. Khaiyer, 2008.: *Journal of Atmospheric and Oceanic Technology*, **25**, Issue 6, 1034–1040, DOI: 10.1175/2007JTECHO546.1

Wang, H, and, R.T. Pinker, 2009: Shortwave radiative fluxes from MODIS: Model development and implementation. *JGR-Atmopsheres*, **114**, D20201.

Wonsick, M. M., R.T. Pinker and Yves Govaerts, 2009: Cloud Variability over the Indian Monsoon Region as Observed from Satellites. *JAMC*, **48** (9), 1803-1821.

Wood, E., and Coauthors, 1998: The Project for Inter-comparison of Land-Surface Parameterization Schemes (PILPS) Phase2(c) Red-Arkansas River basin experiment: 1.

Experiment description and summary inter-comparisons. *Global Planet. Change,* **19,** 115–135.

Wu, W.-S., R. J. Purser, and D. F. Parrish, 2002: Three-dimensional variational analysis with spatially inhomogeneous covariances. Mon. Wea. Rev., 130,2905–2916, doi:10.1175/1520-0493(2002)130<2905:TDVAWS>2.0.CO;2.

Xue, Y., P. J. Sellers, J. L. Kinter, and J. Shukla, 1991: A simplified biosphere model for global climate studies. *J. Climate,* **4,** 345–364.